Bioactive Materials 6 (2021) 1867–1877

Contents lists available at ScienceDirect

Bioactive Materials

journal homepage: www.sciencedirect.com/journal/bioactive-materials

Myocardial protection by heparin-based coacervate of FGF10

Zhouguang Wang [a,b,c,1], Yan Huang [a,b,1], Yan He [d,1], Sinan Khor [c], Xingxing Zhong [c], Jian Xiao [a,b], Qingsong Ye [e,g,*], Xiaokun Li [a,b,f,**]

[a] School of Pharmacy, Key Laboratory of Biotechnology and Pharmaceutical Engineering, Wenzhou Medical University, Wenzhou, 325035, China
[b] Engineering Laboratory of Zhejiang Province for Pharmaceutical Development of Growth Factors, Biomedical Collaborative Innovation Center of Wenzhou, Wenzhou, Zhejiang, 325035, China
[c] Department of Molecular Pharmacology, Albert Einstein College of Medicine, Bronx, NY, 10461, USA
[d] Laboratory of Regenerative Medicine, Tianyou Hospital, Wuhan University of Science and Technology, Wuhan, 430064, China
[e] Centre of Regenerative Medicine, Renmin Hospital of Wuhan University, Wuhan, 430060, China
[f] Research Units of Clinical Translation of Cell Growth Factors and Diseases Research, Chinese Academy of Medical Science, China
[g] School and Hospital of Stomatology, Wenzhou Medical University, Wenzhou, 325035, China

ARTICLE INFO

Keywords:
Fibroblast growth factor-10
Angiogenesis
Controlled release
Myocardial infarction
Coacervate

ABSTRACT

Heart disease is still the leading killer all around the world, and its incidence is expected to increase over the next decade. Previous reports have already shown the role of fibroblast growth factor10 (FGF10) in alleviating heart diseases. However, FGF10 has not been used to treat heart diseases because the free protein has short half-life and low bioactivity. Here, an injectable coacervate was designed to protect growth factor from degradation during delivery and the effects of the FGF10 coacervate were studied using a mice acute myocardial infarction (MI) model. As shown in our echocardiographic results, a single injection of FGF10 coacervate effectively inhibited preserved cardiac contractibility and ventricular dilation when compared with free FGF10 and the saline treatment 6 weeks after MI. It is revealed in histological results that the MI induced myocardial inflammation and fibrosis was reduced after FGF10 coacervate treatment. Furthermore, FGF10 coacervate treatment could improve arterioles and capillaries stabilization through increasing the proliferation of endothelial and mural cells. However, with the same dosage, no statistically significant difference was shown between free FGF10, heparin+FGF10 and saline treatment, especially in long term. On another hand, FGF10 coacervate also increased the expression of cardiac-associated the mRNA (cTnT, Cx43 and α-SMA), angiogenic factors (Ang-1 and VEGFA) and decreased the level of inflammatory factor (tumor necrosis factor-α). The downstream signaling of the FGF10 was also investigated, with the western blot results showing that FGF10 coacervate activated the *p*-FGFR, PI3K/Akt and ERK1/2 pathways to a more proper level than free FGF10 or heparin+FGF10. In general, it is revealed in this research that one-time injection of FGF10 coacervate sufficiently attenuated MI induced injury when compared with an equal dose of free FGF10 or heparin+FGF10 injection.

1. Introduction

Despite decades of research, coronary heart disease (CHD) is still the leading cause of death and disability worldwide [1–3]. Myocardial infarction (MI) is one serious result of CHD which is characterized by myocardial necrosis, chronic inflammation and the generation of fibrotic scar tissue. The cell death and subsequent pathological remodeling in myocardial infarction zone finally result in heart failure [4]. Novel therapies for myocardial infarction have been widely investigated, which include pro-angiogenic growth factors, stem cell and ECM treatment [5–7]. Although researches and pre-clinical studies have demonstrated the pharmacological roles of pro-angiogenic factors in improving MI [8,9], they have failed to show appreciable effects in the final clinical trials [10–12]. The main reason is that the knowledge of blood vessels formation, the body's endogenous responses to ischemic injury, growth factor selection and/or the timing that growth factors

* Corresponding author. Centre of Regenerative Medicine, Renmin Hospital of Wuhan University, Wuhan, 430060, China.
** Corresponding author. School of Pharmacy, Key Laboratory of Biotechnology and Pharmaceutical Engineering, Wenzhou Medical University, Wenzhou, 325035, China.
E-mail addresses: qingsongye@hotmail.com (Q. Ye), lixk1964@163.com (X. Li).
[1] These authors contributed equal to this study.

https://doi.org/10.1016/j.bioactmat.2020.12.002
Received 4 September 2020; Received in revised form 18 November 2020; Accepted 1 December 2020

reach the target zone is limited. The last but not least, the pharmacological functions of growth factors are significantly reduced via direct injection *in vivo* since proteolytic degradation and enzymatic deactivation happen in very short time after intervention. In our recent research, an injectable biodegradable and biocompatible coacervate was designed to deliver the heparin-binding growth factors, which effectively reduced the degradation and inactivation of fibroblast growth factor 10 (FGF10) during delivery.

In this study, a controlled delivery system containing a natural polyanion and poly (ethylene argininylaspartate diglyceride) (we named it as PEAD), a heparin and a biodegradable polycation was designed. All these parts form a complex coacervate via the charge interaction between them. The polycation and polyanion bind together as a neutral complex, encapsulating the heparin-binding proteins. Thus, the proteins are separated from the surrounding aqueous environment and protected from degradation. Studies on utilization of this heparin-based coacervate delivery system have been widely performed. It has been used to deliver growth factors including fibroblast growth factor-1 (FGF1), nerve growth factor [13–15], heparin-binding epidermal growth factor-like growth factor [16] and so on [17,18] and the enhanced effects of growth factors on MI were revealed when using coacervate as the delivery system [19].

FGF10 is one of the FGF family members mainly synthesized by mesenchymal cells. It is a key player in lung development and fetal limb, prostatic epithelial cell growth and skin wound healing. Previous studies have shown that FGF10 is one of the major markers of the early cardiac progenitor cells and play an important role in proliferation of differentiated cardiomyocytes in developing embryo [20]. Moreover, reduced FGF10 expression has been revealed in mouse postnatal heart. During this period, cardiomyocytes exit the cell cycle, following with the loss of regenerative capacities. All these researches suggest that FGF10 is important for heart regeneration. However, the overexpression of FGF10 in the neonatal mouse heart cannot increase post-natal cardiac regeneration [21]. Nevertheless, the effect of FGF10 on inducing cardiomyocyte cell-cycle re-entry under physiological conditions suggests that FGF10 might play an important role in cardiomyocyte renewal in injured hearts [20]. However, growth factors have not been used in the clinical treatment of heart disease because of the short half-lives and low bioactivity when directly injected *in vivo* [22]. Interestingly, free FGF10 exhibited a higher bioactivity when combined with heparin [23]. Here, in this article, the coacervate delivery system was used to increase the half-life and promote the bioactivity of FGF10. Then the potential of FGF10 to decrease cardiac fibrotic process and promote cardiac function after MI injury was investigated.

2. Materials and methods

2.1. The preparation of FGF10 coacervate

FGF10 coacervate was prepared using PEAD and heparin [14,24]. Briefly, Heparin and PEAD were dissolved in deionized water separately to achieve a final concentrations of 10 mg/ml. FGF10 and heparin were mixed at first, followed by PEAD to have the coacervate formed. The clear solution turning to turbid indicated the successful formation of coacervate. The final mass ratios of FGF10: heparin: PEAD were 1:100:500.

The *in vitro* release profile of the FGF10 coacervate was investigated [15]. Briefly, 200 μl of FGF10 coacervate (included 500 ng of FGF10) suspended in saline was centrifuged at the speed of 10,000 rpm for 10 min then stored at 37 °C. The supernatant was aspirated on day 0, 1, 4, 7, 10, 14 and 21 and stored at −80 °C, then the pellet was covered by adding 200 μl saline solution. ELISA (R&D Systems, MN) was used to measure the released FGF10 in each fraction per time point.

Dynamic light scattering was used to measure the size of coacervate. PEAD and Heparin were separately dissolved in deionized water then mixed at a mass ratio 5:1 PEAD: heparin. A Zetasizer Nano ZS machine was used to measure the size of coacervate droplet.

2.2. Cell proliferation and migration measurement in vitro

Human umbilical vein endothelial cells (HUVEC) from ATCC were cultured in EBM-2 media. After washed with DMEM, the cells were added with nutrient-deprived media without supplements, vehicle, free FGF10 (50 ng/ml), heparin+FGF10 (50 ng/ml) or FGF10 coacervate (50 ng/ml), then incubated at 37 °C for 72 h. After wash, Aqueous One Solution (Cell Titer 96® Cell Proliferation Assay purchased from Promega) was added and incubated in 5% CO_2 at 37 °C for 3 h. The absorbance was read at 490 nm.

Transwell chemotaxis experiment was used to test the effect of FGF10 coacervate on the migration of HUVEC. Cells were seeded at a density of 10,000 cells/cm^2 in transwell (24-well) which was inserted with 8 μm pore size. Nutrient-deprived media without supplements, vehicle, free FGF10 (50 ng/ml), heparin+FGF10 (50 ng/ml) or FGF10 coacervate (50 ng/ml) were added to the well. After 12 h' incubation, non-migrated cells were cleaned with cotton swabs and migrated cells were fixed in methanol. After 10 min, Quant-iT Pico Green dsDNA reagent (Thermo Fisher Scientific, P7581) was used to have migrated cells stained. Fluorescent images were taken using Nikon Eclipse Ti fluorescence microscope and the NIS-Elements AR imaging software. Three independent images from three different areas were taken for cells number quantification. To analyze the cell number, each group was normalized to the average number of cells in the vehicle group individually.

2.3. Acute myocardial infarction model (MI) and intramyocardial injection in mouse

9–12 weeks old male C57/B6 mice were maintained in compliance with the Institutional Animal Care and Use Committee of Wenzhou Medical University. The mice were sacrificed for sample collection at different time points after treatment [5,15]. The left coronary artery of the mice was ligated to induce MI. Five minutes after inducting the MI, different treatments including 35 μl saline, free FGF10 (500 ng of FGF10), heparin+FGF10 (100 μg of heparin and 500 ng of FGF10) or FGF10 coacervate (500 μg of PEAD, 100 μg of heparin and 500 ng of FGF10) was administered. These different treatments were injected across three different sites of the ischemic area of myocardium (the center and the bilateral border zones of the infarct area). The final FGF10 dose used in this study was selected according to our pilot experiment and previous studies [15]. All procedures and injections were double blind.

2.4. Echocardiography (echo)

Cardiac function was evaluated using echocardiography before and 5 days, 2 weeks and 6 weeks after MI injury. The heart and respiratory rates were monitored at 37 °C body temperature using a hot pad. A high frequency linear probe with the Vevo 2100 Imaging System was used to measure echocardiographic parameters. Short-axis images of the LV in B-mode were used to measure End-systolic area (ESA) and end-diastolic area (EDA). The definition of FAC was: 100%*(EDA-ESA)/EDA), which correctly reflected contractility of the heart. Ejection fraction of the left ventricle (LVEF) was also calculated. The quantification of *in vivo* strain was using images of short axis B-mode echocardiography from the Vevo Strain software system. Briefly, three mice were analyzed in each group. Circumferential and radial strain within the ventricular wall were measured by speckle-tracking at the injured region. The circumferential and radial strain values at the injured region were normalized to the uninjured region to have the ventricular wall thickness calculated, which was then compared to healthy cardiac tissue in the same heart.

2.5. Histological stains

The hearts of mice were harvested 2 and 6 weeks after MI injury. The hearts were frozen in OCT for further staining. Hearts were sectioned from apex to the ligation level using a cryostat. The section thickness was 8 μm. The thickness of the ventricular wall in the infarct area was measured using ImageJ software, at the middle of infarcted area. For observation of fibrosis, collagen fibers were staining using Masson's trichrome kit. Images from each treatment group (ten sections per group) were taken to have scar condition examined through the ventricle wall. All the measurements were performed 6 weeks after MI.

2.6. Immunofluorescent staining

Serum from appropriate species was used to block the tissue. After penetrated with 0.3% Triton-X 100, sections were incubated with primary antibodies including rat anti-mouse CD68 (Abcam, Cambridge, MA), FITC-conjugated monoclonal antibody against α-SMA (Sigma Aldrich, St. Louis, MO) and rat anti-mouse CD31 (BD Biosciences, San Jose, CA). Samples were then incubated with appropriate secondary antibody (Alexa Fluor 488 or 555) at RT for 1 h. Naïve IgGs of the appropriate species were included as negative controls. DAPI nuclear staining was utilized to reveal the cells in tissue sections. A fluorescence microscope (Nikon Eclipse Ti) and AR imaging software (Nikon NIS-Elements) were used to take images. Three to six sections of different mouse hearts in each treatment group were included for data analysis. All the measurements were taken as cells per mm^2 area. For *in vivo* degradation test, multi-photon excitation (MPE) imaging was conducted. Briefly, rhodamine labeled ulex europaeus agglutinin-1 was mixed with heparin before PEAD was added into the solution containing [heparin:rhodamine] complexes to form coacervate. Free or heparin-bound rhodamine-ulex europaeus agglutinin-1 or rhodamine-ulex europaeus agglutinin-1 coacervate (dilute in 30 μl of 0.9% saline) was delivered through intramyocardial injections after MI. Hearts were harvested 21 days after injection. MPE images were captured using an Olympus multiphoton microscope.

2.7. Western blot analysis

The mice were sacrificed 28 days after myocardial infarction injury. The hearts were homogenized in a RIPA buffer, the equivalent of 50 μg of protein was separated on 10% gel and then transferred to a PVDF membrane. After blocked with 5% fat-free milk, the membranes were incubated with the relevant protein antibodies overnight. The membranes were washed with TBST then treated with secondary antibodies for 2 h at room temperature. Protein extracts were separated by SDS-PAGE and detected using immunoblotting with antibodies against *anti*-Phospho-FGF Receptor, phospho-ERK1/2, ERK, phospho-AKT, AKT and β-actin (Cell Signaling). Horseradish peroxidase-conjugated anti-rabbit or anti-mouse secondary antibodies (Pierce) was added. Intensity of specific blots was analyzed using image J (version 1.51 and 1.52).

2.8. Statistical analysis

All data are presented as mean ± S.E.M. Samples were randomly assigned to different treatment groups. When experiments contained more than two groups, data were analyzed using analysis of variance and one-way ANOVA Turkey' post hoc analyses. When experiments involved only two groups, data were analyzed using Student's t-test. Software Excel and GraphPad Prism were used for statistical analyses. $P < 0.05$ is regarded as statistically significant.

3. Results

3.1. Characterization of FGF10 coacervate

As shown in the preparation process of FGF10 coacervate (PEAD-heparin-FGF10). (Fig. 1A), both heparin-FGF10 and PEAD had excellent solubility in aqueous solution. After mixed with PEAD, the transparent heparin-FGF10 solution became turbid. 24 h later, FGF10 coacervates aggregate and settle at the bottom of the tube as an oil droplet (shown as white arrow). Because the sulfates of heparin carry negative charges, PEDA and heparin form a coacervate via charge interaction. Moreover, FGF10 contains a binding site that has high affinity to heparin. Thus, PEAD, heparin and FGF10 self-assemble as a ternary complex. FGF10 was fluorescently labeled in green, and the average size of coacervate droplet is 421.6 ± 97.3 nm (Fig. 1B–D). In order to measure the release profile of FGF10 *in vitro*, ELISE was performed at Day 0, 1, 4, 7, 10, 14 and 21. After centrifugation, around 10% FGF10 was detected in the supernatant at day 0. Thus, the loading efficiency of FGF10 for coacervate was around 90%. During the first day, 20.1 ± 3.5% of FGF10 was released. The total amount of FGF10 released by coacervate over the 21-day duration was estimated to be 80.2 ± 4.7% (Fig. 1E). Taken together, it is revealed that FGF10 was stably released by coacervate at a rate of 3.34% per day after the initial burst. In order to mimic the interactions between FGFR-heparin-FGF, a synthetic polycation was used to substitute the heparin-binding sequence of the FGF receptor and a ternary complex containing the polycation, heparin and FGF was formed (Fig. 1F). To evaluate the duration of coacervate *in vivo* post-injection, the multi-photon excitation imaging was performed to detect the degradation of intramyocardially injected rhodamine-tagged coacervate (Coa-Rho). Indicated by our quantification of the fluorescence volume, Coa-Rho showed high fluorescent volume within the infarct area 7 days after injection. In contrast, few fluorescent signaling was detected after injected with free (Free-Rho) or heparin rhodamine (Hep-Rho) (Fig. 1H). 21 days after injection, the red fluorescent signaling was detected in Coa-Rho group but not in free or heparin groups (Fig. 1G). The results above suggest a progressive degradation of coacervate *in vivo* for at least 21 days after intracardiac injection.

3.2. FGF10 coacervate induces human umbilical vein endothelial cell chemotaxis and proliferation

An *in vitro* experiment was performed to investigate the proliferation effect of FGF10 coacervate on HUVEC. 50 ng/ml of FGF10, heparin+FGF10 or FGF10 coacervate was selected as the treatment concentration according to our previous studies [15]. It is revealed that 50 ng/ml of free FGF10 or heparin+FGF10 treatment did not lead to increase of HUVEC proliferation when compared with vehicle group ($p > 0.05$) (Fig. 2A). However, FGF10 coacervate significantly increased HUVEC proliferation when compared with free FGF10 ($p < 0.05$), heparin+FGF10 ($p < 0.05$) and vehicle treatment ($p < 0.01$) (Fig. 2A). A transwell experiment was conducted to evaluate chemotaxis induced by FGF10 coacervate on HUVECs. Enhanced chemotaxis of HUVECs was revealed after the treatment of FGF10 coacervate, an equal dose of free FGF10 or heparin+FGF10 when compared with basal media treatment (free FGF10 or heparin+FGF10: $p < 0.05$; FGF10 coacervate: $p < 0.01$) (Fig. 2B–C). Notably, chemotactic effects induced by FGF10 coacervate was greater than induced by an equal dose of free FGF10 or heparin+FGF10 ($p < 0.001$) (Fig. 2B–C). No statistical difference of the effects on cell migration was revealed between the basal media treated group and the vehicle group ($p > 0.05$). To summarize, it is indicated that FGF10 released from the coacervate has highly bioactivity in stimulating the migration and proliferation of HUVECs *in vitro*.

3.3. The protective effect of FGF10 coacervate on cardiac structure

To further elucidate how FGF10 coacervate affects the structure of

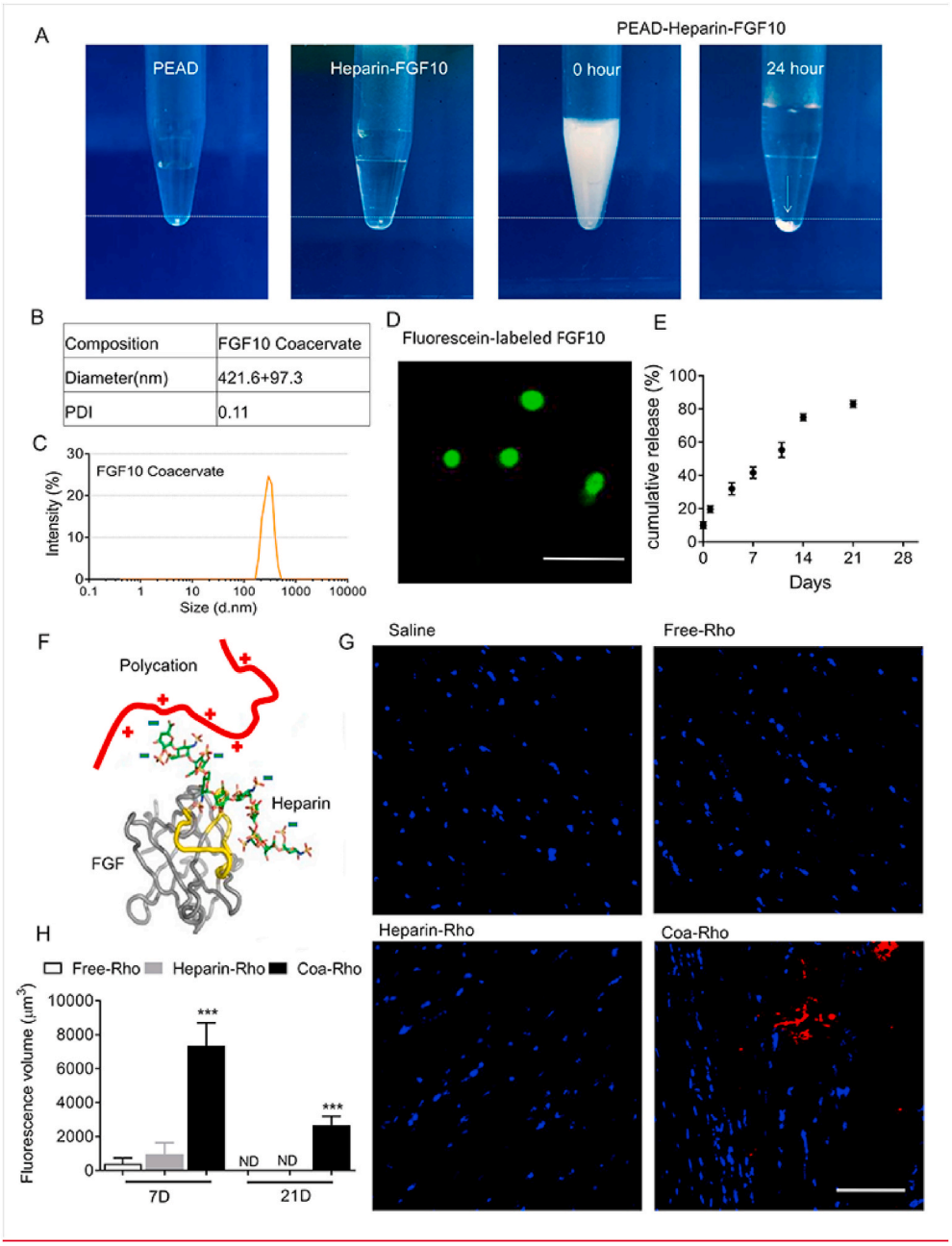

Fig. 1. The controlled release of FGF10 through coacervate delivery system. (A) The preparation of FGF10-coacervate. The precipitation particles are labeled with white arrow. (B–C) The quantified diameter and the polydispersity index (PDI) of coacervate. (D) Representative image of immunofluorescent stained FGF10. Bar = 5 μm. (E) ELISA result showing the *in vitro* release profile of FGF10 coacervate for 21 days. Data are shown as cumulative percentage release. (F) The schematic showing the design of the coacervate. A synthetic polycation replaces the heparin-binding domain of FGFR and forms a complex together with heparin and FGF. The heparin-binding domains of FGF is highlighted in yellow. (G) Representative MPE images of the ischemic hearts 21 days after injected with saline, Free-Rho, Hep-Rho or Coa-Rho. (H) The quantification of fluorescence volume in ischemic hearts of saline, Free-Rho, Hep-Rho, or Coa-Rho group at Day 7 or 21 after injection. *** represents $p < 0.001$ vs Free-Rho or Hep-Rho group. Error bars represent mean ± S.E.M. (For interpretation of the references to colour in this figure legend, the reader is referred to the Web version of this article.)

the heart, the infarct regions were stained 6 weeks after myocardial infarction injury (Fig. 3A). As shown in saline-treated group, the infarcted area has thin ventricle wall and dilated ventricle when compared with a normal heart. The normal myocardial tissue was replaced by granulation and scar. In free FGF10 or heparin+FGF10 treatment animals, the area of infarcted cardiac tissue was reduced. However, the condition of fibers and tissue architecture damage was not obviously different in comparison to the saline-treated group. In contrast, FGF10 coacervate was shown to have effects on improving infarcted damage and preserving a normal size of ventricle (Fig. 3B). As a result (Fig. 3C), increased thickness of LV wall in the infarcted zone was observed after animals were treated with the FGF10 coacervate (210.8 ± 61.6 μm) but not after treated with free FGF10 (148.6 ± 68.2 μm, $p < 0.05$), heparin+FGF10 (157.6 ± 32.4 μm, $p < 0.05$) and saline (112.6 ± 36.2 μm, $p < 0.01$). Collectively, a role of FGF10 coacervate in reducing the infarct size and preventing ventricular dilation was indicated.

3.4. FGF10 coacervate decrease fibrosis and systemic inflammation induced by myocardial infarction

To examine the condition of collagen deposition in the infarcted myocardium, the tissue was treated using Masson's trichrome stain 6 weeks after MI injury. Consistent with previous studies, significant fibrotic deposition was observed in the infarcted area after MI injury (Fig. 3A) which was present in the border area of ventricular wall in saline-treated animals (Fig. 3A). In the free FGF10 or heparin+FGF10 group, the condition of fibrosis formation was similar to the saline group. In contrast, the scar formation and collagen deposition were reduced in the tissue from the FGF10 coacervate group. The role of FGF10 coacervate in reducing collagen and fibrosis suggested it beneficial effects on enhancing cardiac contractility after MI injury in a long term.

In addition to cardiac fibrosis, local and systemic inflammation is another feature of MI. In this study, phagocytic cells within the infarcted

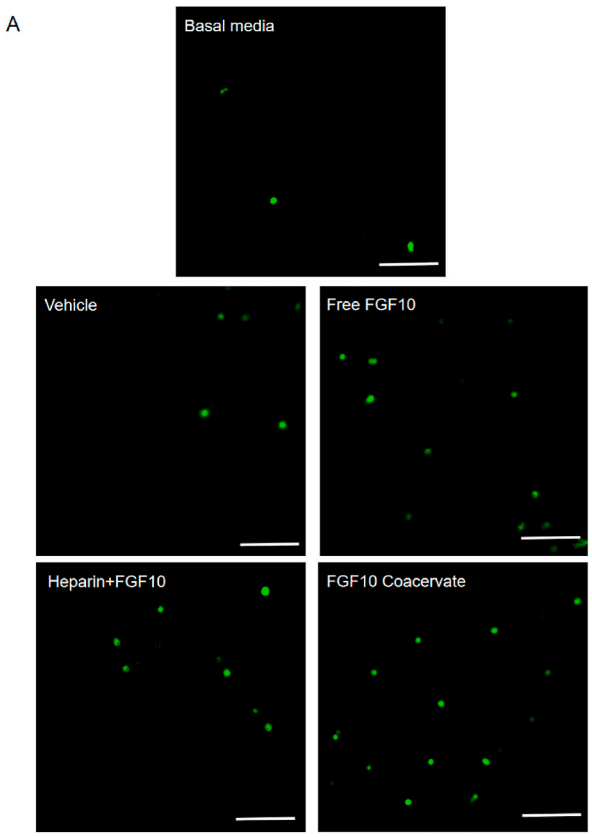

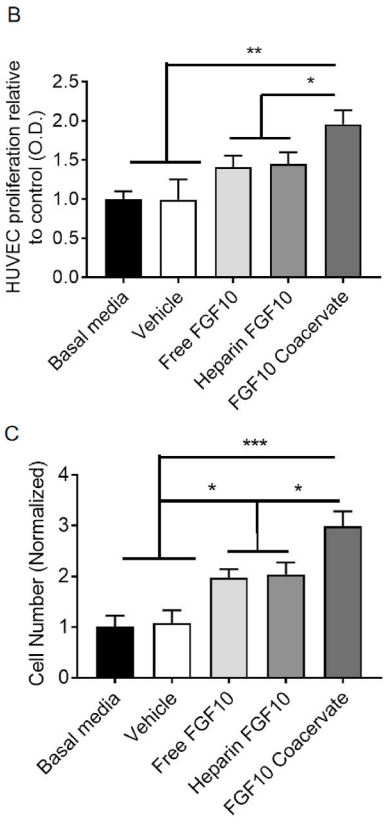

Fig. 2. The effects of FGF10 coacervate on the proliferation and migration of human umbilical vein endothelial cells. (A) Immunofluorescent images of a transwell chemotaxis assay showing the response of human umbilical vein endothelial cells to basal media, vehicle, free FGF10, heparin+FGF10 and FGF10 coacervate treatment. (B) Quantification of HUVEC proliferation data in response to different treatment. (C) Quantification of HUVEC migration data in response to different treatment (n = 4 per group). * represents $p < 0.05$, ** represents $p < 0.01$. Data are represented as mean ± S.E.M.

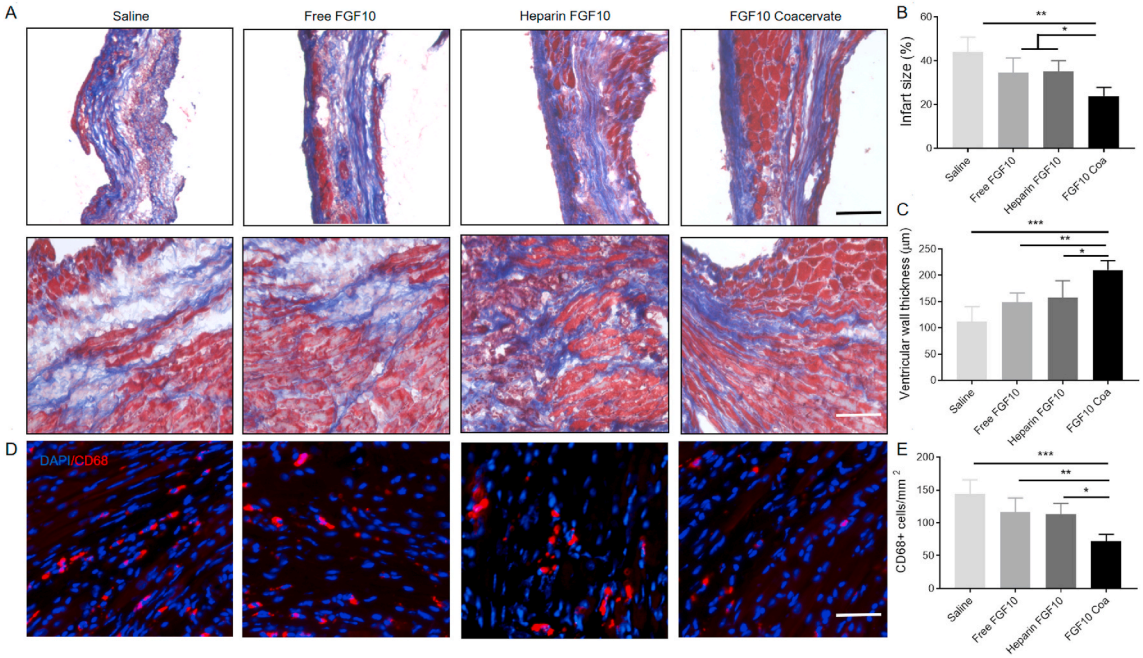

Fig. 3. FGF10 coacervate mitigates inflammation, fibrosis and MI-associated injury. (A) Fibrosis in the infarct and border area was examined using Masson's trichrome staining 6 weeks after MI. Scale bars = 50 μm. Images of the first and second row showing collagen deposition in the border and infarct zones of different groups. (B–C) Quantitative results of infarct size and ventricular wall thickness in different treatment groups. (D) CD68 staining showing the distribution of macrophages in the infarct and border zone 2 weeks after MI injury. Scale bars = 50 μm. (E) Quantitative results of $CD68^+$ cells in saline, free FGF10, heparin+FGF10 and FGF10 coacervate groups. * represents $P < 0.05$, ** represents $P < 0.01$, relative to saline group, free FGF10 or heparin+FGF10 group. All quantitative bars are represented as mean ± S.E.M.

area were stained using CD68 Immunofluorescence 2 weeks after MI. Few $CD68^+$ cells were revealed in normal myocardium while a large number of $CD68^+$ cells were detected in the infarcted myocardium (Fig. 3D). After treated with FGF10 coacervate, numbers of $CD68^+$ cells were reduced while macrophage density was not affected (Fig. 3D). As indicated by quantification results, the $CD68^+$ cell density was not significantly different between the saline, free FGF10 and heparin+FGF10 groups ($p > 0.05$) (Fig. 3E). However, cells expressing $CD68^+$ decreased in FGF10 coacervate treatment group ($p < 0.001$ when compared with saline, $p < 0.05$ when compared with free FGF10 or heparin+FGF10 group) (Fig. 3D–E). Taken together, our results suggest that the macrophage infiltration induced by MI injury in the infarcted area was improved by FGF10 coacervate treatment.

3.5. FGF10 coacervate promotes angiogenesis in mice with myocardial infarction

In the ischemic environment induced by MI, vascularization plays a key role in restoring blood flow, improving myocardial regeneration and recovering heart function. The endothelial cell CD31 marker and vascular smooth muscle cells α-SMA marker were immunofluorescent stained 6 weeks after MI to investigate the vasculature formation in infarct area. In the infarcted zone (Fig. 4A), cells expressing CD31 were barely detected in the saline-treated tissue, and the cell numbers of saline group, free FGF10 group and heparin+FGF10 were not statistically different ($p > 0.05$). Interestingly, cells expressing CD31 increased after the FGF10 coacervate treatment (saline: $p < 0.01$; free FGF10 or heparin+FGF10: $p < 0.05$) (Fig. 4B, D), which suggested a role of the FGF10 coacervate in improving neovessel formation after MI. On another hand, endothelial and mural cells were stained using α-SMA and CD31 to evaluate the vessel formation (including arterioles formation). As a result, few cells expressing α-SMA were detected in the saline-treated tissues 6 weeks after MI injury (Fig. 4A). The number of α-SMA+ cells in saline control revealed no significant difference with the free FGF10 or heparin+FGF10 ($p > 0.05$). However, the FGF10 coacervate treatment group significantly increased the α-SMA+ cells number (saline control: $p < 0.01$; free FGF10: $p < 0.05$) (Fig. 4C, E). To sum up, FGF10 coacervate was reveal to promote angiogenesis in infarcted area when compared with saline and equal dose of free FGF10 or heparin+FGF10.

3.6. FGF10 coacervate improves cardiac function after MI injury

As shown in the echocardiography results, saline treatment mice showed enlargement of the left ventricle at diastole with a high level of EDA (Fig. 5A, F). However, this effect was significantly decreased in mice administrated with FGF10 coacervate treatment 6 week after MI injury ($p < 0.05$ when compared with saline control group 2 weeks after MI, $p < 0.01$ when compared with saline control, free FGF10 or heparin+FGF10 group 6 weeks after MI). A similar trend was observed in the end systolic area (ESA) ($p < 0.01$ when compared with saline, free FGF10 or heparin+FGF10 group 6 weeks after MI) (Fig. 5B). On another hand, it is indicated by fractional area change (FAC), fractional shortening (FS) and ejection fraction (EF) that the cardiac contractile significantly declined in saline treatment group. No significant improvement in FAC, FS and EF was revealed in Free FGF10 or heparin+FGF10 treatment group 6 weeks after MI injury. However, in the FGF10 coacervate treatment group, a remarkable increase in these three parameters was observed when compared with saline control, free FGF10 or heparin+FGF10 group both 2 and 6 weeks after MI (FAC: $p < 0.01$ when compared to saline control, free FGF10 or heparin+FGF10 6 weeks after MI; EF: $p < 0.05$ when compared with saline, free FGF10 or heparin+FGF10 2 and 6 weeks after MI; FS: $p < 0.05$ when compared with saline, free FGF10 or heparin+FGF10 2 weeks after MI, $p < 0.01$ when compared with saline, free FGF10 or heparin+FGF10 6 weeks after MI) (Fig. 5C–E). Taken together, it is suggested by the above results that FGF10 coacervate could maintain both the native function and dimension of the heart 6 weeks after MI injury when compared with saline or free FGF10 treatment.

3.7. FGF10 coacervate amends elasticity which induced by MI injury

To evaluate the mechanical effects of the myocardium, radial and circumferential strain were measured using echocardiography. The strain was measured at the infarcted area of mouse at week 6 after myocardial injury then normalized to the strain values with the ventricle wall of non-infarcted areas (Fig. 6A). Six weeks after MI injury, both circumferential and radial strain values at the infarct region of saline, free FGF10, heparin+FGF10 and FGF10 coacervate groups were lower than the uninjured group (Fig. 6B–D), which was due to the scar formation in the infarcted area. It is revealed that saline treatment group exhibited lowest circumferential and radial strain values in all three groups. Free FGF10 or heparin+FGF10 treatment was shown to increase circumferential and radial strain values a bit but without statistically significance when compared to saline group ($p > 0.05$). In contrast, FGF10 coacervate treatment was shown to significantly increase strain values when compared with saline, Free FGF10 and heparin+FGF10 groups ($p < 0.01$ when compared with saline; $p < 0.05$ when compared with Free FGF10 or heparin+FGF10) (Fig. 6B and C). To sum up it is

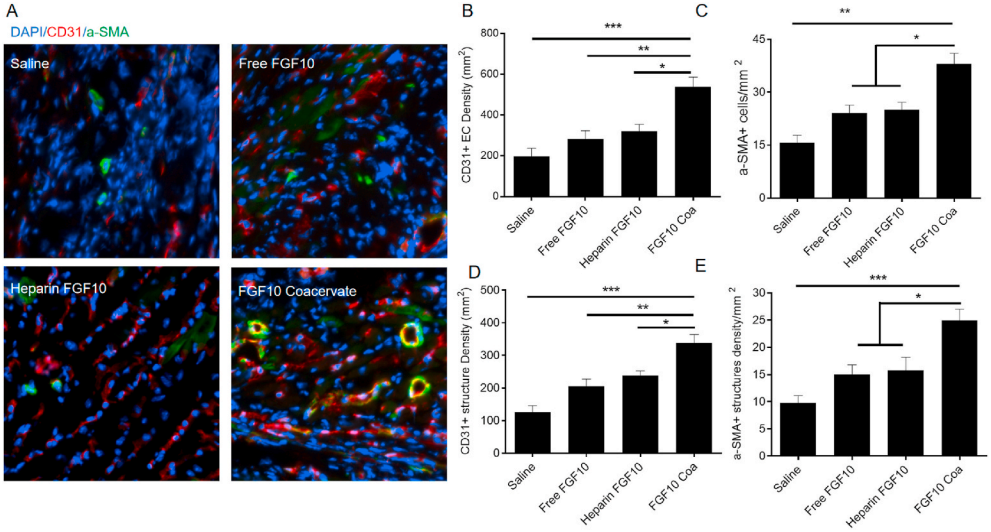

Fig. 4. FGF10 coacervate promote vascular stabilization in the infarcted area. (A) CD31 and α-SMA staining in the infarcted area. Quantification of $CD31^+$ (B) and α-SMA+ (C) cells showing increased density of vascular endothelial cells in response to FGF10 coacervate treatment. The quantitative results of CD31 positive blood vessels (D) and blood vessels surrounded by α-SMA-expressing cells (E). *$p < 0.05$, **$P < 0.01$, ***$P < 0.001$, related to saline, free FGF10 or heparin+FGF10 group. All quantitative bars are represented as mean ± S.E.M.

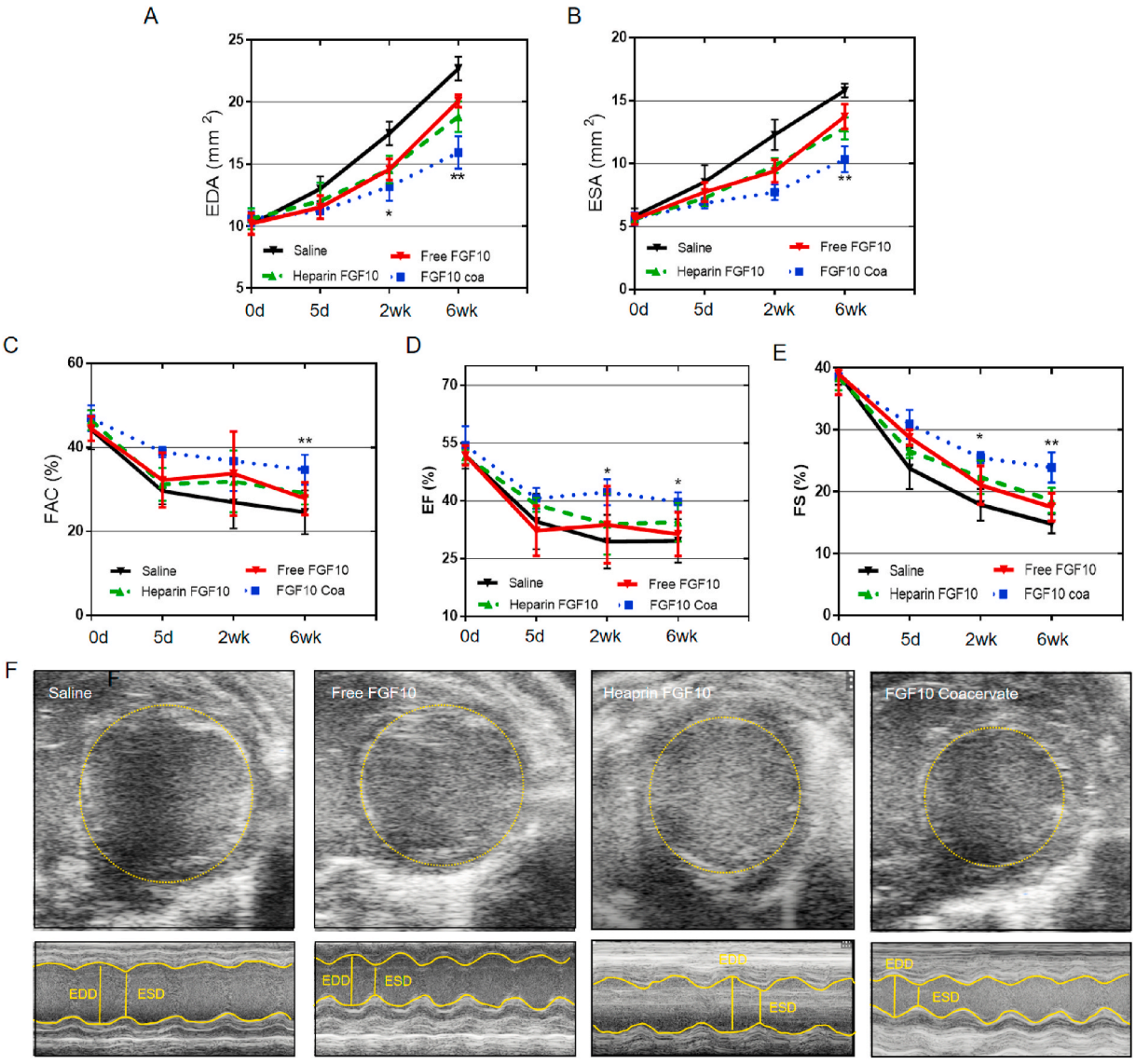

Fig. 5. Echocardiographic results showing the improved cardiac function after FGF10 coacervate treatment. (A) The EDA and (B) ESA results of mice 5 days, 2 weeks and 6 week after the treatment of saline, free FGF10 and FGF10 coacervate. (C) FGF10 coacervate treatment significantly increased FAC when compared with saline or free FGF10 groups 6 weeks after MI injury. The EF (D) and FS (E) results of mice 5 days, 2 weeks and 6 weeks after the treatment of saline, free FGF10, heparin+FGF10 and FGF10 coacervate. (F) Representative echocardiography images in M-mode and B-mode of different groups 6 weeks after MI injury. *P < 0.05, **P < 0.01 compared with saline, free FGF10 or heparin+FGF10. All quantitative bars are represented as mean ± S.E.M.

suggested that FGF10 coacervate was involved in restoring or preserving left ventricle myocardial elasticity after myocardial injury.

3.8. *The gene expression suggests the protective role of the FGF10 coacervate in MI injury*

FGF10 has cardioprotective role in MI injury via various physiological processes including reducing inflammatory and stimulating angiogenesis. Furthermore, FGF10 has been reported to involve in promoting cardiomyocyte proliferation. To confirm the cardioprotective effects of FGF10 released from coacervate on treating myocardial infarction, the mRNA expression of tumor necrosis factor alpha (TNF-α) and proangiogenic growth factors (Ang-1 and VEGFA) in the infarct area were tested using RT-PCR. It is revealed in Fig. 7A that FGF10 coacervate significantly decreased the mRNA level of TNF-α but increased the gene level of Ang-1 and VEGFA when relative to saline, free FGF10 or heparin+FGF10 group (Fig. 7 B, C). It might be due to effects of FGF10 coacervate on increasing cell survival and reversing the unfavorable microenvironment in the infarct area. The data above shows that FGF10 coacervate promoted angiogenesis, reduced inflammatory and further helped the cardiac function restoration, which is consistent with the histology and immunofluorescence staining results. Connexin 43 (Cx43) is known as a connexin that contributes to the myocardial cell-to-cell connection [25]. In order to evaluate the electroactivity effects after myocardial injury, the gene expression of connexin 43 (Cx43) was tested. As revealed in Fig. 7D, the gene expression of connexin 43 (Cx43) was significantly increased after FGF10 coacervate treatment. To evaluate the heart functions after treatment of saline, free FGF10, heparin+FGF10 and FGF10 coacervate, cTnT and α-SMA were tested (Fig. 7E and F). The gene expression of cTnT and α-SMA was detected in the infarct area after myocardial injury, however, the mRNAs level of cTnT and α-SMA was upregulated after FGF10 coacervate treatment. The upregulation cTnT mRNA level helps to support the cardioprotective effects of FGF10 coacervate after MI injury.

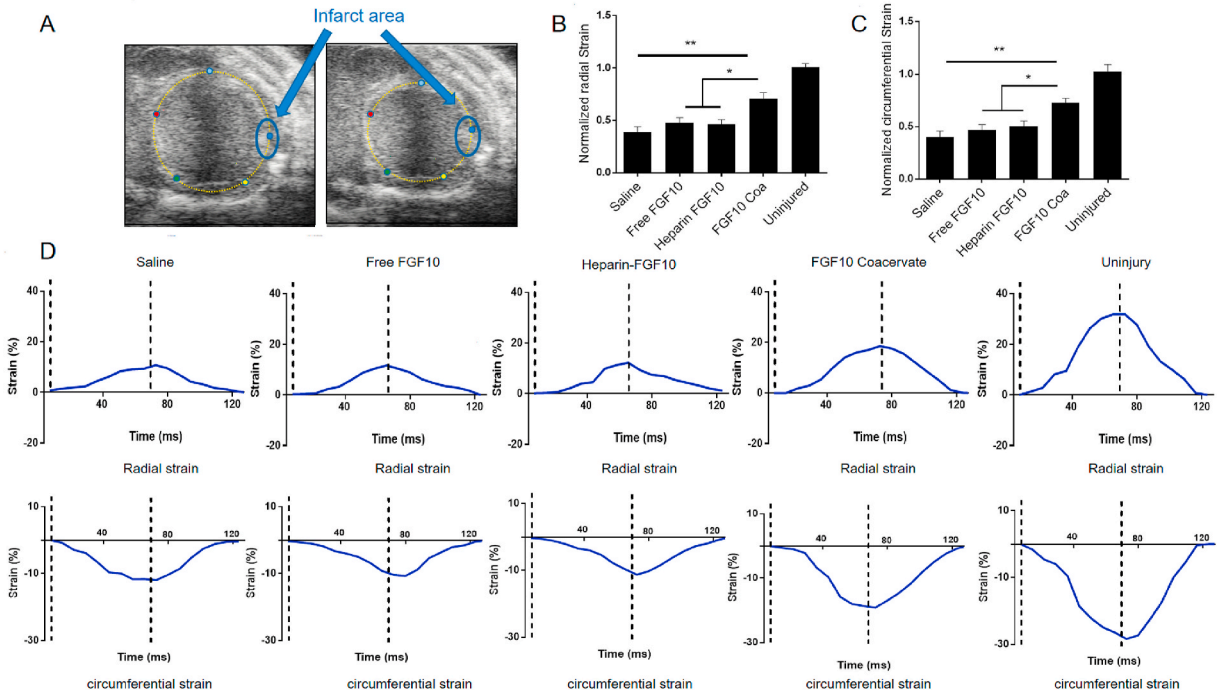

Fig. 6. The analysis of myocardial strain in response to different treatment (A) Representative images of B-mode echocardiography, the infarct area is labeled as blue circle. Quantification results of radial (B) and circumferential (C) strain in response to saline, free FGF10, heparin+FGF10 and FGF10 coacervate treatment. (D) Representative graphs showing radial and circumferential strain of infarcted area after the treatment of saline, free FGF10 and FGF10 coacervate (n = 4; * represents $p < 0.05$, ** represents $p < 0.01$ relative to saline, free FGF10 or heparin+FGF10 groups). All quantitative bars are represented as mean ± S.E.M. (For interpretation of the references to colour in this figure legend, the reader is referred to the Web version of this article.)

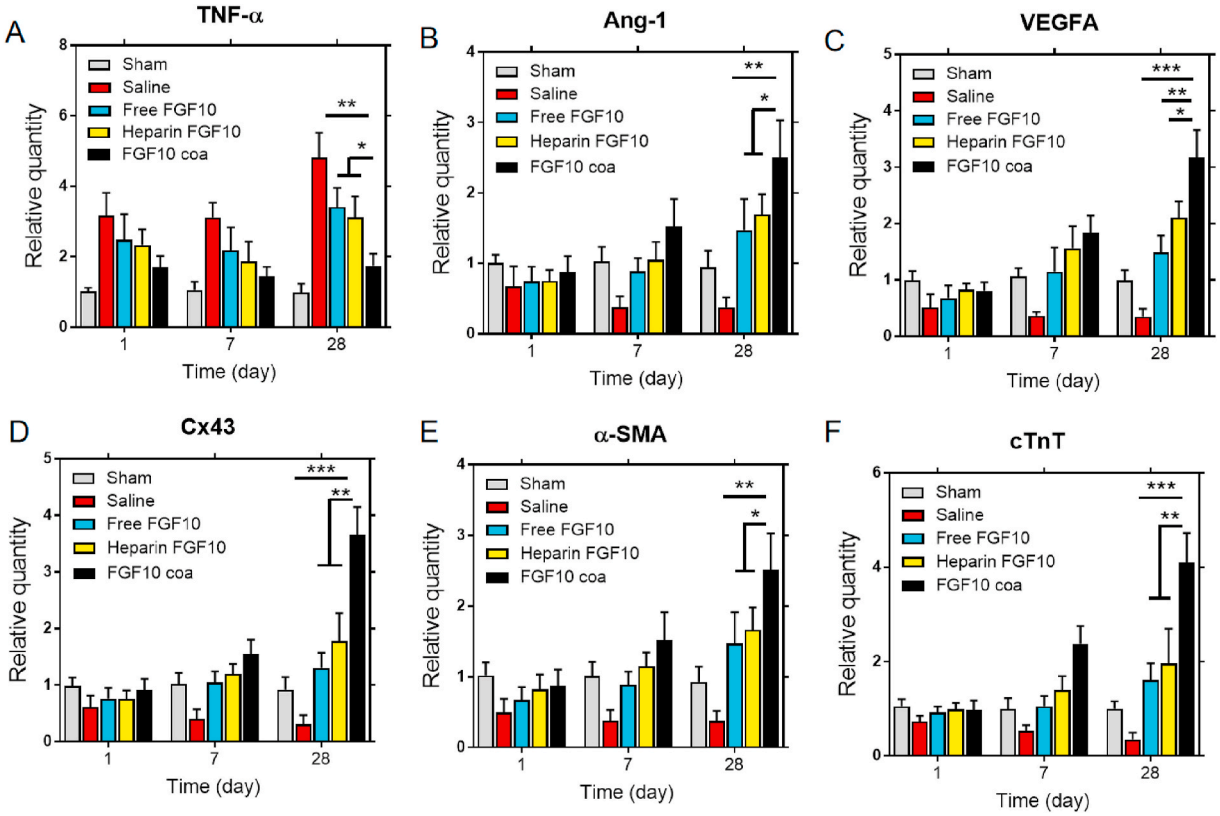

Fig. 7. RT-PCR results showing different gene expression. (A–F) The mRNAs level of TNF-α, Ang-1, VEGFA, Cx43, cTnT, and α-SMA 1, 7 and 28 day after different treatment (n = 6 per group; * represents $p < 0.05$, ** represents $p < 0.01$ and *** represents $p < 0.001$ relative to saline, free FGF10 or heparin+FGF10 groups). All quantitative bars are represented as mean ± S.E.M.

3.9. FGF10 coacervate could increase cardiomyocyte survival via activation of the PI3K/Akt and ERK1/2 pathways

As we know, the viability of the cardiac muscle plays an important role in the heart functions. Cardiomyocytes are cells making up of the cardiac muscle and involved in the heart contractile function. Myocardial infarction injury leads to massive death of cardiomyocytes, so promoting the survival and preventing the apoptosis of cardiomyocytes is important in the treatment of MI. Indicated by cTnT immunofluorescence staining results (Fig. 8A), a major loss of viable myocardium was observed in the saline, free FGF10 and heparin+FGF10 groups. After treated with FGF10 coacervate, the live cardiomyocytes were apparently preserved to a large extent at Day 28. In addition, a dramatically decreased viability of the cardiac muscle was shown in saline-treated animal (Fig. 8B). Both free FGF10 and heparin FGF10 treatment were able to increase the density of survived cardiomyocytes. However, the effect of FGF10 coacervate on maintaining the survival of the cardiac muscle was significantly better than saline, free FGF10 and heparin FGF10 groups (Fig. 8B). Various molecular pathways have been shown to play important roles in promoting survival after MI, e.g., (phosphorylated) ERK1/2 and Akt pathways. Here in our research, western blotting was used to investigate the protein expression of the FGF10 receptor, FGF10 downstream *p*-ERK1/2 and *p*-Akt 28 days after injury. Increased *p*-ERK1/2 and *p*-AKT/AKT level were observed in free FGF10 ($P < 0.05$), heparin FGF10 ($P < 0.05$) and FGF10 coacervate-treated ($P < 0.001$) groups, with a highest expression level revealed in the FGF10 coacervate-treated group (Fig. 8C, E). Collectively, FGF10 coacervate was revealed to improve the long-term survival of cardiomyocytes after MI injury via activating the PI3K/Akt and ERK1/2 pathways.

4. Discussion

The beneficial roles of proangiogenic factors in cardiac function have been regarded as a novel approach to improve myocardial blood flow [26,27] and the improved angiogenesis and revascularize ischemic myocardium have been revealed in pre-clinical MI models after treated with proangiogenic factors [28,29]. However, the effects of proangiogenic factors in treating MI in clinical trials are disappointing. For example, in Phase I and II clinical trials, FGF1, PDGF, GM-CSF, VEGF, neuregulin-1, hepatocyte growth factor, and FGF2 therapies showed limited effects on promoting revascularization and improving heart function, despite being reasonably safe and tolerable at the different doses used [30,31]. One of the major reasons is that the half-life of free protein is short. Another reason is that the bioavailability of systemically delivered growth factors varies, which depends on the availability of vasculature in target tissue. To improve therapeutic efficacy, frequent administration and high doses of growth factors were utilized. However,

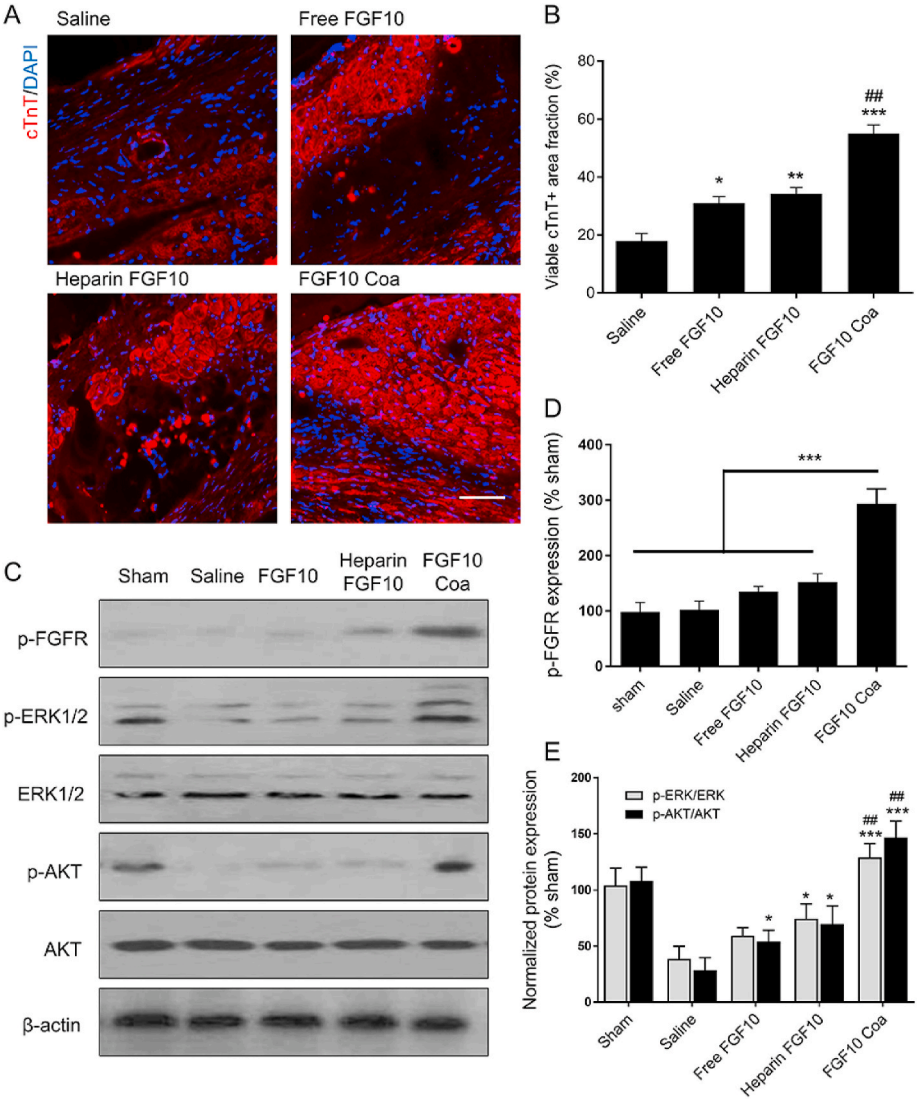

Fig. 8. Effects of FGF10 coacervate on cardiomyocyte survival via activating PI3K/Akt and ERK1/2 pathways. (A) Representative cardiac troponin T (cTnT) immunofluorescence staining images of the different treatment groups 28 days after MI injury. (B) The quantitative analysis of the cTnT protein expression level at Day 28 after MI injury. (C) Representative western blot images showing the expression level of *p*-FGFR, *p*-ERK1/2, ERK, *p*-AKT and AKT in different groups 28 days after injury. (D) A bar diagram of phospho-FGFR levels of western blot bind analyses. Actin was used as a protein loading control and for band density normalization. (E) A bar diagram of phospho-Akt/Akt and phosphorylated-ERK/ERK level of western blot bind analyses. * represents $p < 0.05$, ** represents $p < 0.01$ and *** represents $p < 0.001$ relative to saline, ## represents $p < 0.01$ relative to saline free FGF10 or heparin+FGF10 groups. All quantitative bars are represented as mean ± S.E.M.

systemic toxicity might be caused by a high dose of the protein. For example, it is shown in a previous study that intracoronary infusing a high dose (50 ng/kg/min) of VEGF in MI patients caused nitric oxide-mediated hypotension [11]. Hence, to solve these problems, a suitable controlled release system that can improve the bioavailability of exogenous growth factors during delivery is urgently needed.

Here, a coacervate comprised of heparin and a polycation PEAD was used as a delivery system. Heparin is a negatively charged and has high affinity to more than 400 bioactive proteins and peptides including extracellular matrix (ECM) proteins, growth factors and cytokines. These inter-molecular interactions in a large extent depend on the basic amino acid residues (lysine, histidine and arginine) on the proteins' heparin-binding domain, and these residues are also important to activating the downstream pathway [32]. In our coacervate, the heparin is immobilized non-covalently via electrostatic interactions, which makes its natural bioactivity well preserved [33]. In addition, Heparin facilitates the binding of FGF10 and its receptor. The protein is isolated from aqueous environment by coacervate phase separation and subsequently protected from rapid degradation [34]. Limited cytotoxicity is exhibited by this biodegradable polyester, regardless of its cationic charge [24]. This coacervate system has been widely used to deliver protein in treating cardiac damage animal models. For example, Shh exhibited a heart protective role in rodent MI model when delivered using our coacervate. Additionally, FGF-2 delivered using coacervate was shown to benefit angiogenesis after MI [35].

In this study, the roles of FGF10 coacervate in MI injury model was investigated. FGF10 was chosen because its increased activity when bound with heparin [23]. FGF10 was evenly homogeneous incorporated into coacervate droplets with a loading efficiency higher than 90% exhibited. At the first day, a low initial dose of FGF10 (20.1 ± 3.5%) was released. During the next 21 days, FGF10 was stably released with amount of about 15 ng every day. The *in vitro* experiment was conducted to reveal that the proliferation of HUVECs was significantly improved after treated with FGF10 coacervate, but not with free FGF10 or saline. Transwell assays were performed to evaluate the chemotactic effects of HUVEC, which suggested that FGF10 coacervate induced greater chemotactic effects on HUVEC when compared with free FGF10 treatment. Collectively, the bioactivity of FGF10 is highly preserved when delivered with the coacervate and the coacervate delivered FGF10 is shown to have beneficial roles in proliferation and migration of HUVECs *in vitro*.

For the animal study *in vivo*, a mouse myocardial infarction (MI) model was used to investigate the involvement of FGF10 coacervate system in angiogenesis in the infarcted area. After treated with FGF10 coacervate, cells expressing CD31 and α-SMA increased. It suggests the formation of vasculature, which is consistent with the results of *in vitro* experiment. Reduced myocardial fibrosis was also revealed in infarcted areas which improved contractile function damage induced by MI [36]. In addition, the pharmacological function of FGF10 in mediating cardioprotective signaling pathways in cardiomyocytes was suggested [37]. Previous researches have demonstrated that maintaining viable cardiac muscle exhibited a key role in improving cardiac function after MI [38–40]. Moreover, the macrophage was less infiltrated in the infarcted region after the FGF10 coacervate treatment, which could be related to indirect inhibition of pro-inflammatory cytokines. The reduced inflammation could also be a direct result of improved angiogenesis and better-preserved cardiac muscle. Our previous studies in which FGF10 was used to treat spinal cord injury showed similar results that $CD68^+$ and inflammatory M1 macrophages induced by spinal cord injury were reduced. The functional benefits resulted from improvements in cardiac contractility were observed 6 weeks after MI. Putative mechanisms involved in FGF10 coacervate mediated ischemic heart repair have been summarized with a schematic depiction in Supplemental Fig. 1.

Taken together, FGF10 coacervate activated the *p*-FGFR, *p*-ERK1/2 and *p*-AKT to a more proper level than free FGF10 and heparin+FGF10, and higher therapeutic potential was exhibited in FGF10 coacervate treatment in contrast to free FGF10, heparin+FGF10 and saline treatment. Future pre-clinical experiments will be needed to future validate the effects of this therapeutic approach before applying this delivery system in treating patients with ischemic heart diseases. Additional investigations on optimizing therapeutic dose of FGF10 and maximizing the efficacy are also required. Besides, since heparin has a high affinity to a wide range of proteins, studies investigating effects of multiple proteins-bound coacervate in MI model are also worth to perform in the future.

5. Conclusion

In conclusion, it is demonstrated in our study that administrating FGF10 delivered using the coacervate delivery system improves the stabilization and formation of new blood vessels and cardiac function in adult MI mice model. Which further improve cardiac function in adult mice following MI injury. The improvement of cardiac function is observed 2 weeks after MI and reaches a higher level at week 6. Overall, FGF10 delivered using coacervate can activate the downstream of FGF10 signals to a more proper level than free FGF10 and heparin+FGF10, and improved myocardial function in MI mice model via promoting new vessels formation, inhibiting inflammation and decreasing collagen deposition. In the future, studies using large animal models will be conducted to validate the effects of the coacervate in treating ischemic heart diseases.

CRediT authorship contribution statement

Zhouguang Wang: Conceptualization, Methodology, Writing - original draft. **Yan Huang:** Conceptualization, Methodology. **Yan He:** Formal analysis, Writing - review & editing. **Sinan Khor:** Writing - review & editing. **Xingxing Zhong:** Writing - review & editing. **Jian Xiao:** Writing - review & editing. **Qingsong Ye:** Writing - review & editing. **Xiaokun Li:** Funding acquisition, Supervision.

Declaration of competing interest

The authors declare that there is no known conflict of interest that could influence the findings reported in this paper, neither at personal nor at organizational level.

Acknowledgements

This work was supported by grants from Advanced Postdoctoral Programs of Zhejiang (zj2019030), China Postdoctoral Science Foundation (2019M662015). Research Unit of Research and Clinical Translation of Cell Growth Factors and Diseases, Chinese Academy of Medical Science (No.2019RU010 to X.L.) and CAMS Innovation Fund for Medical Sciences (2019-I2M-5-028), China.

Appendix A. Supplementary data

Supplementary data to this article can be found online at https://doi.org/10.1016/j.bioactmat.2020.12.002.

References

[1] F. Sanchis-Gomar, C. Perez-Quilis, R. Leischik, A. Lucia, Epidemiology of coronary heart disease and acute coronary syndrome, Ann. Transl. Med. 4 (13) (2016) 256.
[2] W.C.R.C.W. Group, World Health Organization cardiovascular disease risk charts: revised models to estimate risk in 21 global regions, Lancet Glob. Health 7 (10) (2019) e1332–e1345.
[3] S.S. Virani, A. Alonso, E.J. Benjamin, M.S. Bittencourt, C.W. Callaway, A.P. Carson, A.M. Chamberlain, A.R. Chang, S. Cheng, F.N. Delling, L. Djousse, M.S.V. Elkind, J. F. Ferguson, M. Fornage, S.S. Khan, B.M. Kissela, K.L. Knutson, T.W. Kwan, D. T. Lackland, T.T. Lewis, J.H. Lichtman, C.T. Longenecker, M.S. Loop, P.L. Lutsey, S. S. Martin, K. Matsushita, A.E. Moran, M.E. Mussolino, A.M. Perak, W.D. Rosamond, G.A. Roth, U.K.A. Sampson, G.M. Satou, E.B. Schroeder, S.H. Shah, C.M. Shay, N.

L. Spartano, A. Stokes, D.L. Tirschwell, L.B. VanWagner, C.W. Tsao, E. American Heart Association Council on, C. Prevention Statistics, S. Stroke Statistics, Heart disease and stroke statistics-2020 update: a report from the American heart association, Circulation 141 (9) (2020) e139–e596.
[4] C.M. Orrego, G. Torre-Amione, Is myocardial ischemia the cause of the progressive decrease in ejection fraction during acute decompensated heart failure ? J. Card. Fail. 15 (6) (2009). S27-S27.
[5] Z.G. Wang, D.W. Long, Y. Huang, W.C.W. Chen, K. Kim, Y.D. Wang, Decellularized neonatal cardiac extracellular matrix prevents widespread ventricular remodeling in adult mammals after myocardial infarction, Acta Biomater. 87 (2019) 140–151.
[6] W.C.W. Chen, Z.G. Wang, M.A. Missinato, D.W. Park, D.W. Long, H.J. Liu, X. M. Zeng, N.A. Yates, K. Kim, Y.D. Wang, Decellularized zebrafish cardiac extracellular matrix induces mammalian heart regeneration, Sci. Adv. 2 (11) (2016).
[7] F.R. Formiga, E. Tamayo, T. Simon-Yarza, B. Pelacho, F. Prosper, M.J. Blanco-Prieto, Angiogenic therapy for cardiac repair based on protein delivery systems, Heart Fail. Rev. 17 (3) (2012) 449–473.
[8] Y.D. Tang, F. Hasan, F.J. Giordano, S. Pfau, H.M. Rinder, S.D. Katz, Effects of recombinant human erythropoietin on platelet activation in acute myocardial infarction: results of a double-blind, placebo-controlled, randomized trial, Am. Heart J. 158 (6) (2009) 941–947.
[9] P. Meier, S. Gloekler, S.F. de Marchi, A. Indermuehle, T. Rutz, T. Traupe, H. Steck, R. Vogel, C. Seiler, Myocardial salvage through coronary collateral growth by granulocyte colony-stimulating factor in chronic coronary artery disease A controlled randomized trial, Circulation 120 (14) (2009) 1355–1363.
[10] A.A. Voors, A.M.S. Belonje, F. Zijlstra, H.L. Hillege, S.D. Anker, R.H.J.A. Slart, R. A. Tio, A. Van't Hof, J.W. Jukema, H.O.J. Peels, J.P.S. Henriques, J.M. ten Berg, J. Vos, W.H. van Gilst, D.J. van Veldhuisen, H.I. Investigators, A single dose of erythropoietin in ST-elevation myocardial infarction, Eur. Heart J. 31 (21) (2010) 2593–2600.
[11] T.D. Henry, B.H. Annex, G.R. McKendall, M.A. Azrin, J.J. Lopez, F.J. Giordano, P. K. Shah, J.T. Willerson, R.L. Benza, D.S. Berman, C.M. Gibson, A. Bajamonde, A. C. Rundle, J. Fine, E.R. McCluskey, V. Investigators, The VIVA trial: vascular endothelial growth factor in Ischemia for Vascular Angiogenesis, Circulation 107 (10) (2003) 1359–1365.
[12] M. Simons, B.H. Annex, R.J. Laham, N. Kleiman, T. Henry, H. Dauerman, J. E. Udelson, E.V. Gervino, M. Pike, M.J. Whitehouse, T. Moon, N.A. Chronos, Pharmacological treatment of coronary artery disease with recombinant fibroblast growth factor-2: double-blind, randomized, controlled clinical trial, Circulation 105 (7) (2002) 788–793.
[13] R. Li, J. Wu, Z. Lin, M.R. Nangle, Y. Li, P. Cai, D. Liu, L. Ye, Z. Xiao, C. He, J. Ye, H. Zhang, Y. Zhao, J. Wang, X. Li, Y. He, Q. Ye, J. Xiao, Single injection of a novel nerve growth factor coacervate improves structural and functional regeneration after sciatic nerve injury in adult rats, Exp. Neurol. 288 (2017) 1–10.
[14] H. Chu, N.R. Johnson, N.S. Mason, Y. Wang, A [polycation:heparin] complex releases growth factors with enhanced bioactivity, J. Contr. Release 150 (2) (2011) 157–163.
[15] Z.G. Wang, D.W. Long, Y. Huang, S. Khor, X.K. Li, X. Jian, Y.D. Wang, Fibroblast growth factor-1 released from a heparin coacervate improves cardiac function in a mouse myocardial infarction model, ACS Biomater. Sci. Eng. 3 (9) (2017) 1988–1999.
[16] N.R. Johnson, Y.D. Wang, Controlled delivery of heparin-binding EGF-like growth factor yields fast and comprehensive wound healing, J. Contr. Release 166 (2) (2013) 124–129.
[17] K.W. Lee, N.R. Johnson, J. Gao, Y. Wang, Human progenitor cell recruitment via SDF-1alpha coacervate-laden PGS vascular grafts, Biomaterials 34 (38) (2013) 9877–9885.
[18] N.R. Johnson, M. Kruger, K.P. Goetsch, P. Zilla, D. Bezuidenhout, Y.D. Wang, N. H. Davies, Coacervate delivery of growth factors combined with a degradable hydrogel preserves heart function after myocardial infarction, ACS Biomater. Sci. Eng. 1 (9) (2015) 753–759.
[19] H.K. Awada, N.R. Johnson, Y.D. Wang, Sequential delivery of angiogenic growth factors improves revascularization and heart function after myocardial infarction, J. Contr. Release 207 (2015) 7–17.
[20] F. Rochais, R. Sturny, C.M. Chao, K. Mesbah, M. Bennett, T.J. Mohun, S. Bellusci, R. G. Kelly, FGF10 promotes regional foetal cardiomyocyte proliferation and adult cardiomyocyte cell-cycle re-entry, Cardiovasc. Res. 104 (3) (2014) 432–442.
[21] N. Rubin, A. Darehzereshki, S. Bellusci, V. Kaartinen, C. Ling Lien, FGF10 signaling enhances epicardial cell expansion during neonatal mouse heart repair, J. Cardiovasc. Dis. Diag. 1 (1) (2013).
[22] A. Beenken, M. Mohammadi, The FGF family: biology, pathophysiology and therapy, Nat. Rev. Drug Discov. 8 (3) (2009) 235–253.
[23] V.N. Patel, K.M. Likar, S. Zisman-Rozen, S.N. Cowherd, K.S. Lassiter, I. Sher, E. A. Yates, J.E. Turnbull, D. Ron, M.P. Hoffman, Specific heparan sulfate structures modulate FGF10-mediated submandibular gland epithelial morphogenesis and differentiation, J. Biol. Chem. 283 (14) (2008) 9308–9317.
[24] H. Chu, J. Gao, Y. Wang, Design, synthesis, and biocompatibility of an arginine-based polyester, Biotechnol. Prog. 28 (1) (2012) 257–264.
[25] T.M. Ribeiro-Rodrigues, T. Martins-Marques, S. Morel, B.R. Kwak, H. Girao, Role of connexin 43 in different forms of intercellular communication - gap junctions, extracellular vesicles and tunnelling nanotubes, J. Cell Sci. 130 (21) (2017) 3619–3630.
[26] T. Nagai, I. Komuro, Gene and cytokine therapy for heart failure: molecular mechanisms in the improvement of cardiac function, Am. J. Physiol. Heart C 303 (5) (2012) H501–H512.
[27] C.L. Hastings, E.T. Roche, E. Ruiz-Hernandez, K. Schenke-Layland, C.J. Walsh, G. P. Duffy, Drug and cell delivery for cardiac regeneration, Adv. Drug Deliv. Rev. 84 (2015) 85–106.
[28] V.F.M. Segers, R.T. Lee, Protein therapeutics for cardiac regeneration after myocardial infarction, J. Cardiovasc. Transl. 3 (5) (2010) 469–477.
[29] H. Chu, Y. Wang, Therapeutic angiogenesis: controlled delivery of angiogenic factors, Ther. Deliv. 3 (6) (2012) 693–714.
[30] G. Srinivas, P. Anversa, W.H. Frishman, Cytokines and myocardial regeneration: a novel treatment option for acute myocardial infarction, Cardiol. Rev. 17 (1) (2009) 1–9.
[31] S. Pascual-Gil, E. Garbayo, P. Diaz-Herraez, F. Prosper, M.J. Blanco-Prieto, Heart regeneration after myocardial infarction using synthetic biomaterials, J. Contr. Release 203 (2015) 23–38.
[32] A. Ori, M.C. Wilkinson, D.G. Fernig, A systems biology approach for the investigation of the heparin/heparan sulfate interactome, J. Biol. Chem. 286 (22) (2011) 19892–19904.
[33] H. Chu, J. Gao, C.W. Chen, J. Huard, Y. Wang, Injectable fibroblast growth factor-2 coacervate for persistent angiogenesis, Proc. Natl. Acad. Sci. U. S. A. 108 (33) (2011) 13444–13449.
[34] J.D. Reboucas, N.S. Santos-Magalhaes, F.R. Formiga, Cardiac regeneration using growth factors: advances and challenges, Arq. Bras. Cardiol. 107 (3) (2016) 271–275.
[35] H. Chu, C.W. Chen, J. Huard, Y. Wang, The effect of a heparin-based coacervate of fibroblast growth factor-2 on scarring in the infarcted myocardium, Biomaterials 34 (6) (2013) 1747–1756.
[36] A.M. Segura, O.H. Frazier, L.M. Buja, Fibrosis and heart failure, Heart Fail. Rev. 19 (2) (2014) 173–185.
[37] F. Rochais, R. Sturny, C.M. Chao, K. Mesbah, M. Bennett, T.J. Mohun, S. Bellusci, R. G. Kelly, FGF10 promotes regional foetal cardiomyocyte proliferation and adult cardiomyocyte cell-cycle re-entry, Cardiovasc. Res. 104 (3) (2014) 432–442.
[38] Z. Wang, Y. Wang, J. Ye, X. Lu, Y. Cheng, L. Xiang, L. Chen, W. Feng, H. Shi, X. Yu, L. Lin, H. Zhang, J. Xiao, X. Li, bFGF attenuates endoplasmic reticulum stress and mitochondrial injury on myocardial ischaemia/reperfusion via activation of PI3K/Akt/ERK1/2 pathway, J. Cell Mol. Med. 19 (3) (2015) 595–607.
[39] Z.G. Wang, Y. Wang, Y. Huang, Q. Lu, L. Zheng, D. Hu, W.K. Feng, Y.L. Liu, K.T. Ji, H.Y. Zhang, X.B. Fu, X.K. Li, M.P. Chu, J. Xiao, bFGF regulates autophagy and ubiquitinated protein accumulation induced by myocardial ischemia/reperfusion via the activation of the PI3K/Akt/mTOR pathway, Sci. Rep. 5 (2015) 9287.
[40] M. Wang, G. Zhang, Y. Wang, T. Liu, Y. Zhang, Y. An, Y. Li, Crosstalk of mesenchymal stem cells and macrophages promotes cardiac muscle repair, Int. J. Biochem. Cell Biol. 58 (2015) 53–61.